

Supplementary Information

All Solid Thick Oxide Cathodes Based on Low Temperature

Sintering for High Energy Solid Batteries

Xiang Han^{1,2,4}, Shanyu Wang¹, Yaobin Xu³, Guiming Zhong⁵, Yang Zhou⁶, Bo Liu⁷, Xiaoyu Jiang¹, Xiang Wang³, Yun Li¹, Ziqi Zhang⁴, Songyan Chen⁴, Chongmin Wang³, Yong Yang⁵, Wenqing Zhang⁸, Junlan Wang⁶, Jun Liu^{1,3*}, and Jihui Yang^{1*}

1. Materials Science and Engineering Department, University of Washington, Seattle, WA 98195, USA

2. College of Materials Science and Engineering, Nanjing Forestry University, Nanjing 210037, China

3. Pacific Northwest National Laboratory, Richland, WA 99252, USA

4. Department of Physics, Xiamen University, Xiamen 361005, China

5. State Key Laboratory for Physical Chemistry of Solid Surfaces, Department of Chemistry, Xiamen University, Xiamen 361005, China

6. Department of Mechanical Engineering, University of Washington, Seattle, WA 98195, USA

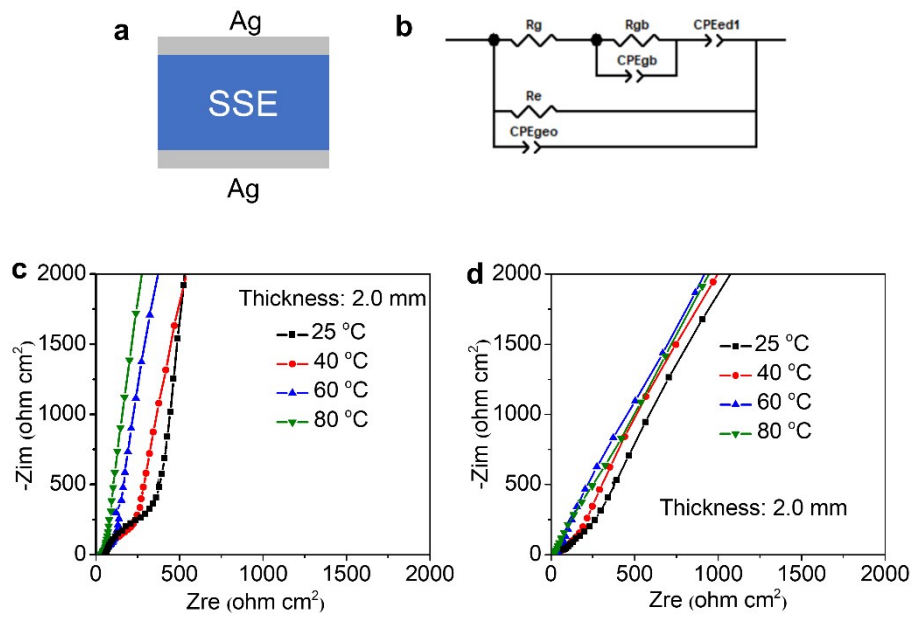
7. Materials Genome Institute, Shanghai University, Shanghai 200444, China

8. Department of Physics, Southern University of Science and Technology, Shenzhen 518055, China

**e-mail: jliu@uw.edu, jihui@uw.edu*

$Al_{0.3}$	a (nm)	c (nm)
0 B_2O_3	0.850	2.080
1 wt. % B_2O_3	0.849	2.081
2 wt. % B_2O_3	0.850	2.084

Supplementary Table 1 Lattice parameters of LABTP with different B_2O_3 contents.



Supplementary Fig. 1 (a) Schematic of the testing pellets with ion-blocking electrodes (Ag). (b) The equivalent circuit with a parallel combination of electronic and ionic resistances, containing a serial combination of bulk resistance (R_b), grain boundary resistance (R_{gb}) with a parallel constant phase element (CPE_{gb}), representing the capacitive behavior of ion-blocking electrodes (Ag). Nyquist plots of (c) LATP (900 °C) and (d) LABTP (750 °C) pellets tested at different temperatures.



$$\Delta G = -7.43 \text{ eV}$$

$$x = 0.1\text{LATP}, \Delta G = -0.124 \text{ eV/LCO}$$



$$\Delta G = -14.93 \text{ eV}$$

$$x = 0.125\text{LATP}, \Delta G = -0.311 \text{ eV/LCO}$$



$$\Delta G = -75.85 \text{ eV}$$

$$x = 0.1316 \text{ LATP}, \Delta G = -0.333 \text{ eV/LCO}$$



$$\Delta G = -16.13 \text{ eV}$$

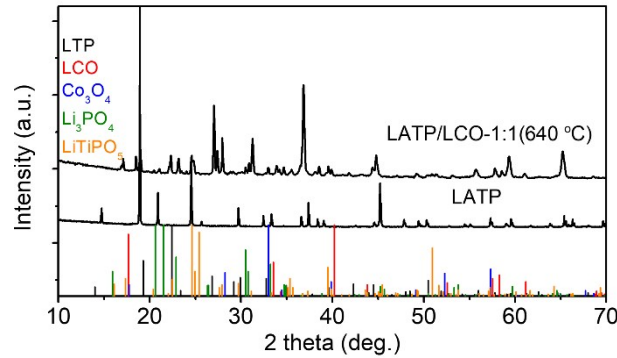
$$x = 0.33 \text{ LATP}, \Delta G = -0.448 \text{ eV/LCO}$$



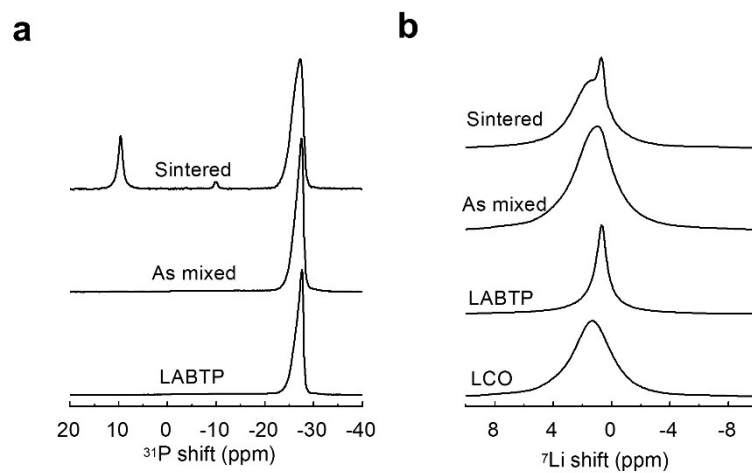
$$\Delta G = -4.75 \text{ eV}$$

$$x = 1 \text{ LATP}, \Delta G = -0.396 \text{ eV/LCO}$$

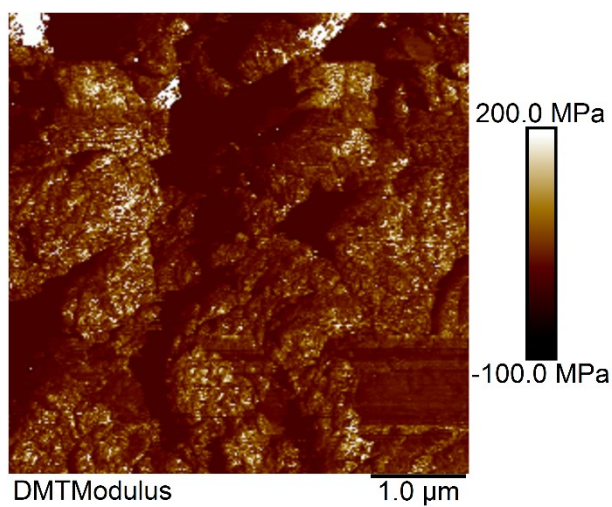
Supplementary Fig. 2 The equations of reactions and the corresponding energetics between LATP and LCO at different molar ratios.



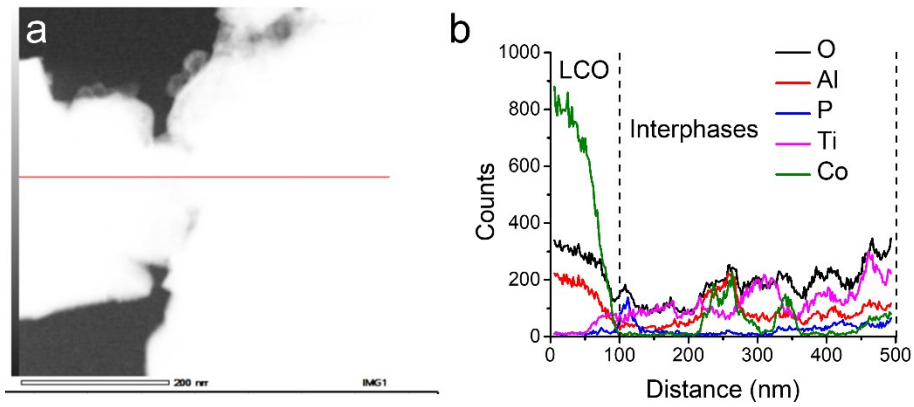
Supplementary Fig. 3 The XRD patterns of the LATP SSE and the LATP/LCO-1:1(640 °C) composite cathode.



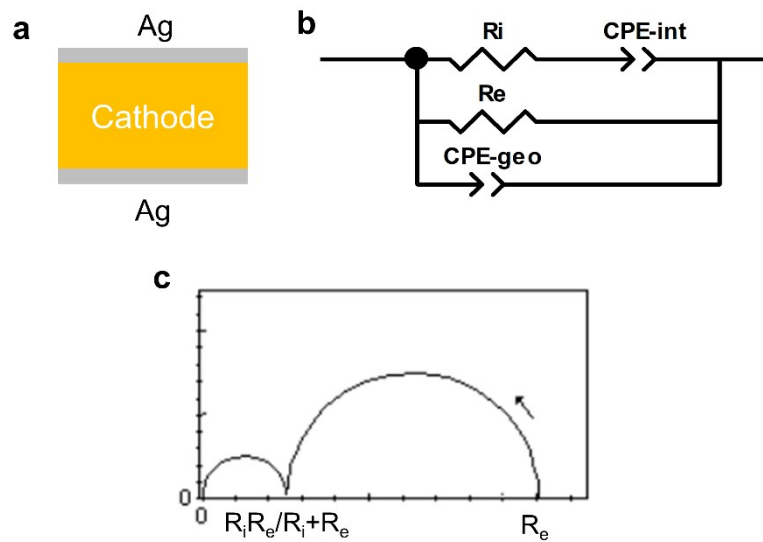
Supplementary Fig. 4 (a) ^{31}P MAS-NMR spectra of LABTP, as-mixed-LABTP/LCO, and sintered-LABTP/LCO-3:7(640 °C). (b) ^7Li MAS NMR spectra of LCO, LABTP, as-mixed-LABTP/LCO, and sintered-LABTP/LCO-3:7(640 °C).



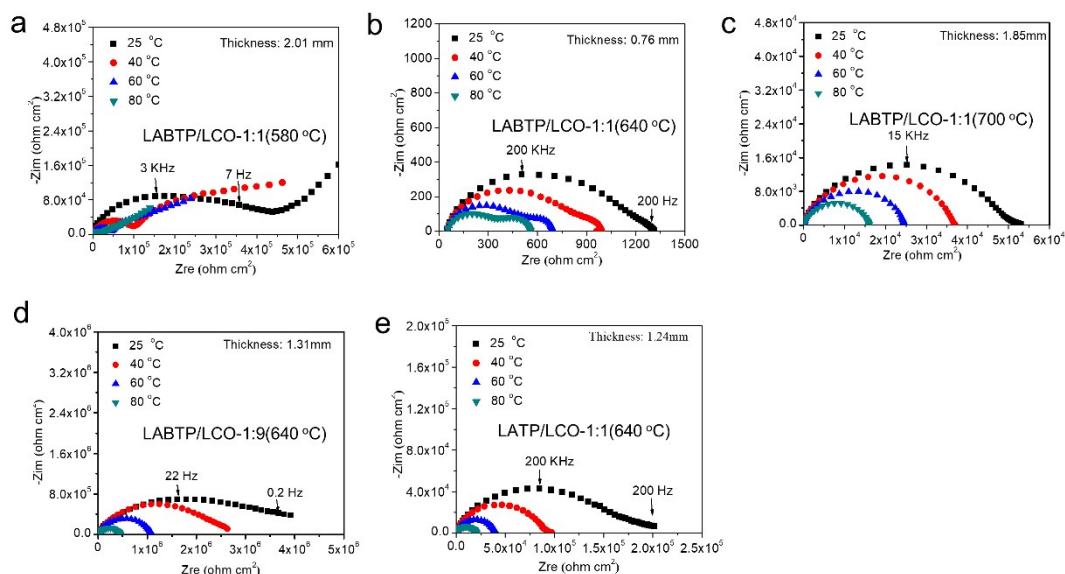
Supplementary Fig. 5 The Derjaguin-Müller-Toporov (DMT) modulus mapping LABTP/LCO sintered at 640 °C.



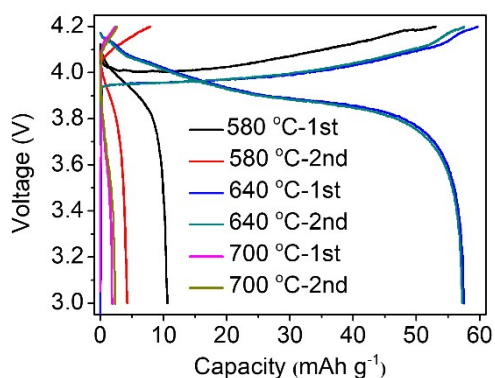
Supplementary Fig. 6 The dark field TEM image of LATP/LCO. (b) EDS line scans for O, Al, P, Ti, and Co.



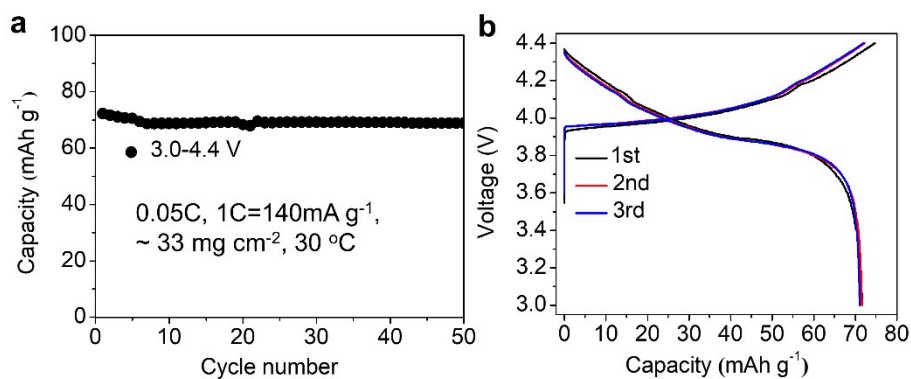
Supplementary Fig. 7 (a) Schematic of the testing pellet with ion-blocking electrodes (Ag). (b) Equivalent circuit of the mixed conductive cathode, in which R_e represents the electronic resistance, R_i the ionic resistance, $CPE-geo$ the geometric capacitance, and $CPE-int$ the interfacial capacitance of the LCO/SSE composite. (c) The simulated curve of EIS test data according to the equivalent circuit in (b).



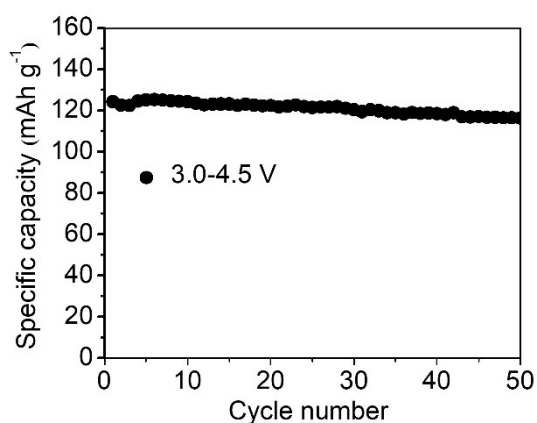
Supplementary Fig. 8 EIS tests of LABTP/LCO composite cathodes. Nyquist plots of (a) LABTP/LCO-1:1(580 °C), (b) LABTP/LCO-1:1(640 °C), (c) LABTP/LCO-1:1(700 °C), (d) LABTP/LCO-1:9(640 °C), and (e) LATP/LCO-1:1(640 °C).



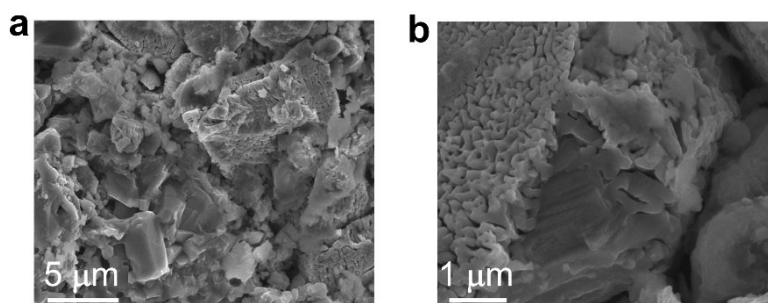
Supplementary Fig. 9 Voltage profiles of LABTP/LCO-1:1 composite cathodes sintered at different temperatures (580, 640, and 700 °C) in semi-solid cells tested at 30 °C in a voltage range of 3.0-4.2 V. The active materials (LCO) loading is $\sim 33 \text{ mg cm}^{-2}$. The charge and discharge rates were set to be 0.05 C (1 C=140 mA g^{-1} , based on the LCO loading).



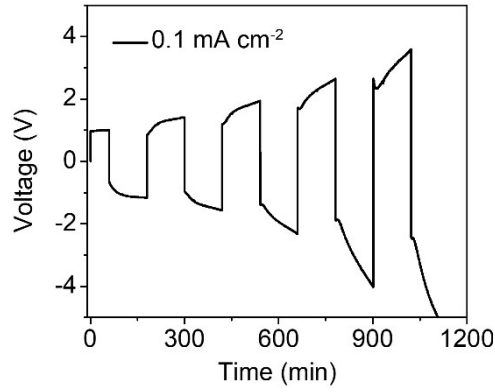
Supplementary Fig. 10 (a) Cycling stability and (b) voltage profiles of LABTP/LCO-1:1(640 °C) composite cathode cycled at 30 °C in a voltage range of 3.0-4.4 V. The active material (LCO) loading is $\sim 33 \text{ mg cm}^{-2}$. The charge and discharge rates were set to be 0.05 C (1 C=140 mA g⁻¹, based on the LCO loading).



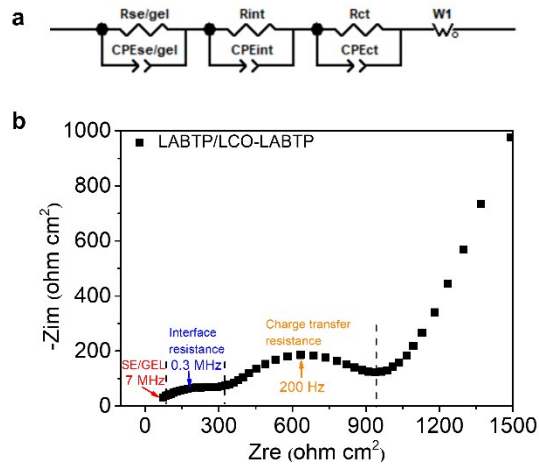
Supplementary Fig. 11 Cycling performance of LABTP/LCO-3:7(640 °C) composite cathode tested at 0.05C (1C=140 mAh g⁻¹) in a wide voltage range of 3.0-4.5 V.



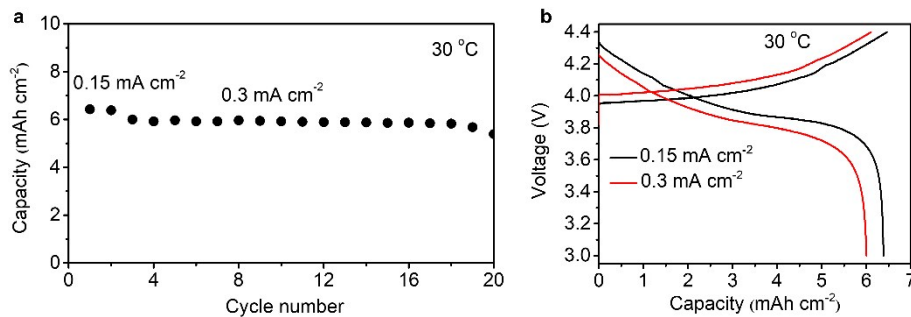
Supplementary Fig. 12 SEM images of LABTP/LCO-1:1(640 °C) after 50 cycles at 0.05C (1C=140 mAh g⁻¹) between cathode in a wide voltage range of 3.0-4.5 V.



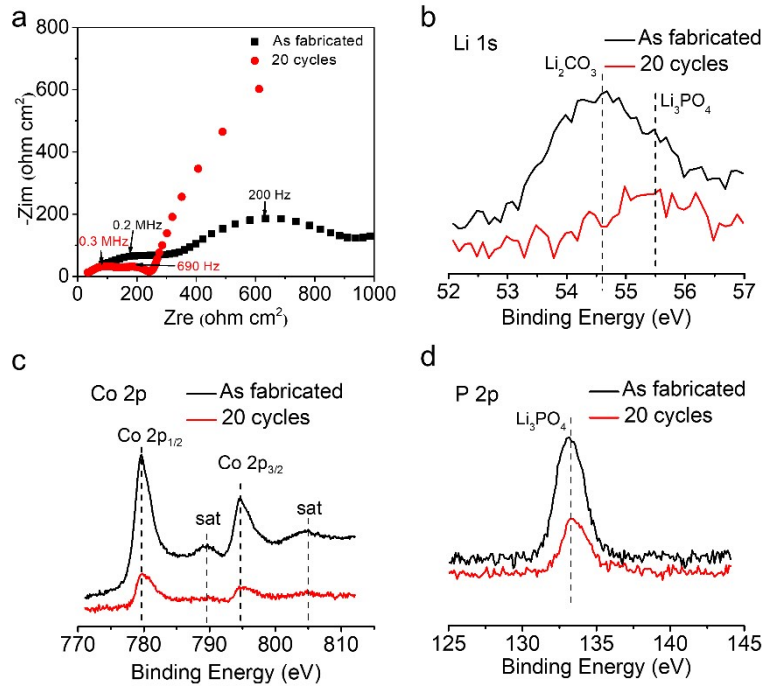
Supplementary Fig. 13 Li-Li symmetric cells with LABTP solid electrolyte (~0.5 mm thick, 10 mm diameter) as separator tested at 60 °C, the current density is 0.1 mA cm⁻².



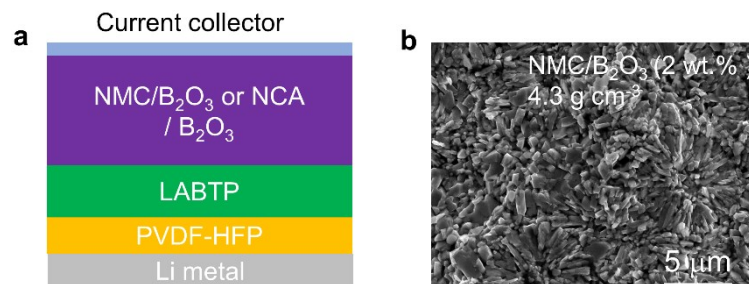
Supplementary Fig. 14 (a) The equivalent circuit for the LABTP/LCO-LABTP solid-state battery. (b) The EIS test data of LABTP/LCO solid-state battery before cycling.



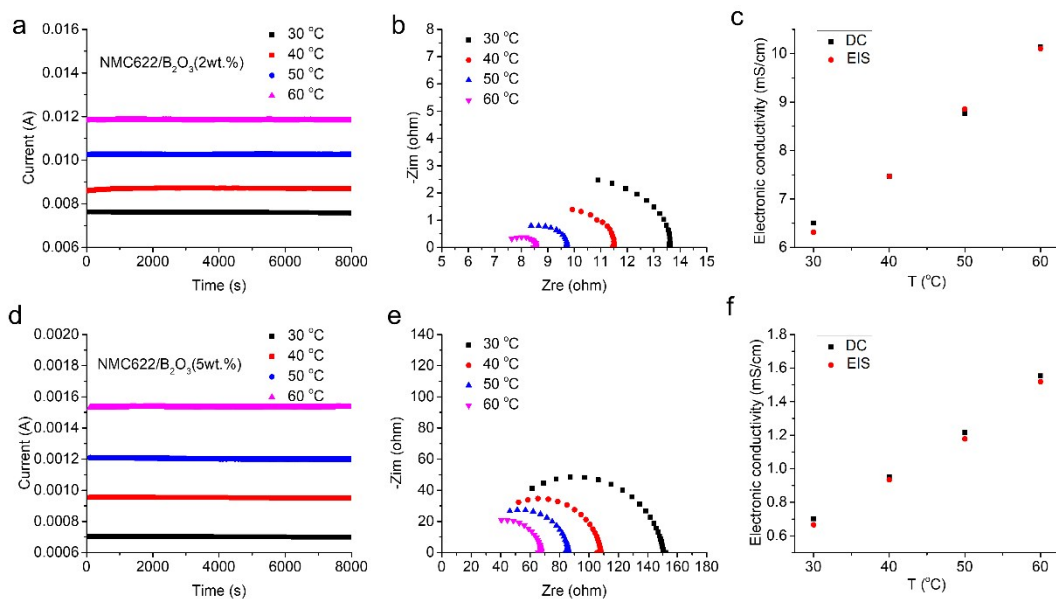
Supplementary Fig. 15 (a) Cycling performance of Li|PVDF-HFP|LABTP|LCO-LABTP battery at 30 °C. (b) Charge-discharge capacity-voltage profiles of Li|PVDF-HFP|LABTP|LCO-LABTP battery at 0.15 and 0.3 mA cm⁻².



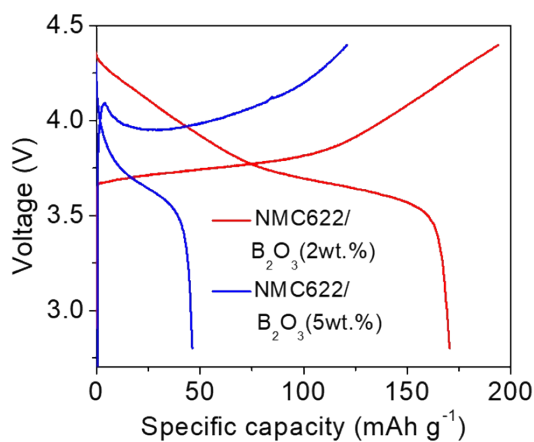
Supplementary Fig. 16 (a) The impedance of LABTP/LCO solid state battery before cycling and after 20 cycles. The XPS data of LABTP/LCO composite cathode before cycling and after 20 cycles: (b) Li 1s, (c) Co 2p, (d) P 2p.



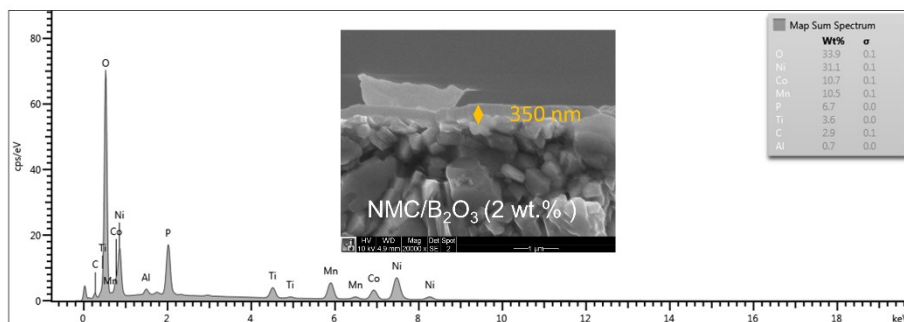
Supplementary Fig. 17 (a) Design of SSBs with LTP SSEs based on liquid phase sintering technique, replacing the LABTP/LCO composite cathodes by NMC/B₂O₃ or NCA/B₂O₃ cathodes could significantly increase the energy density due to higher contents of the active materials, higher energy and higher mass density. (b) A SEM image of the fractured surfaces of the sintered NMC622/B₂O₃ (2 wt.%) cathode, which has a relative high density of 4.3 g cm^{-3} .



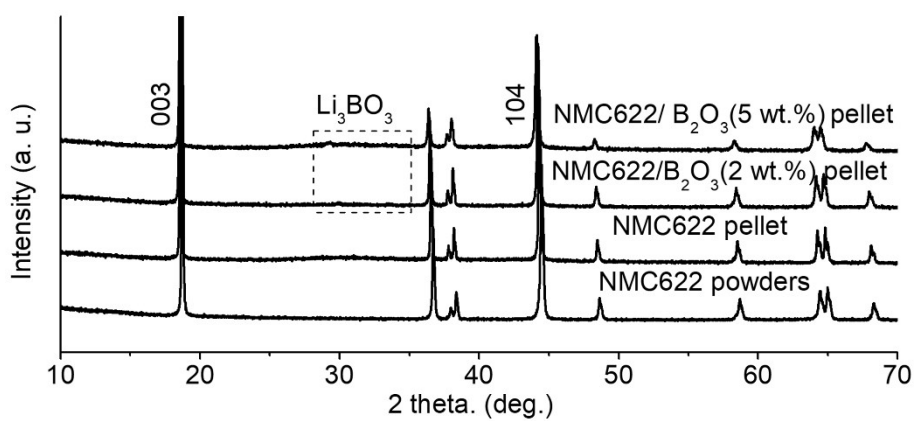
Supplementary Fig. 18 (a) DC measurement of NMC622/B₂O₃(2wt.%) at 30-60 °C. (b) EIS measurement of NMC622/B₂O₃(2wt.%) at 30-60 °C. (c) The calculated electronic conductivity of NMC622/B₂O₃(2wt.%) (d) DC measurement of NMC622/B₂O₃(5wt.%) at 30-60 °C. (e) EIS measurement of NMC622/B₂O₃(5wt.%) at 30-60 °C. (f) The calculated electronic conductivity of NMC622/B₂O₃(5wt.%)



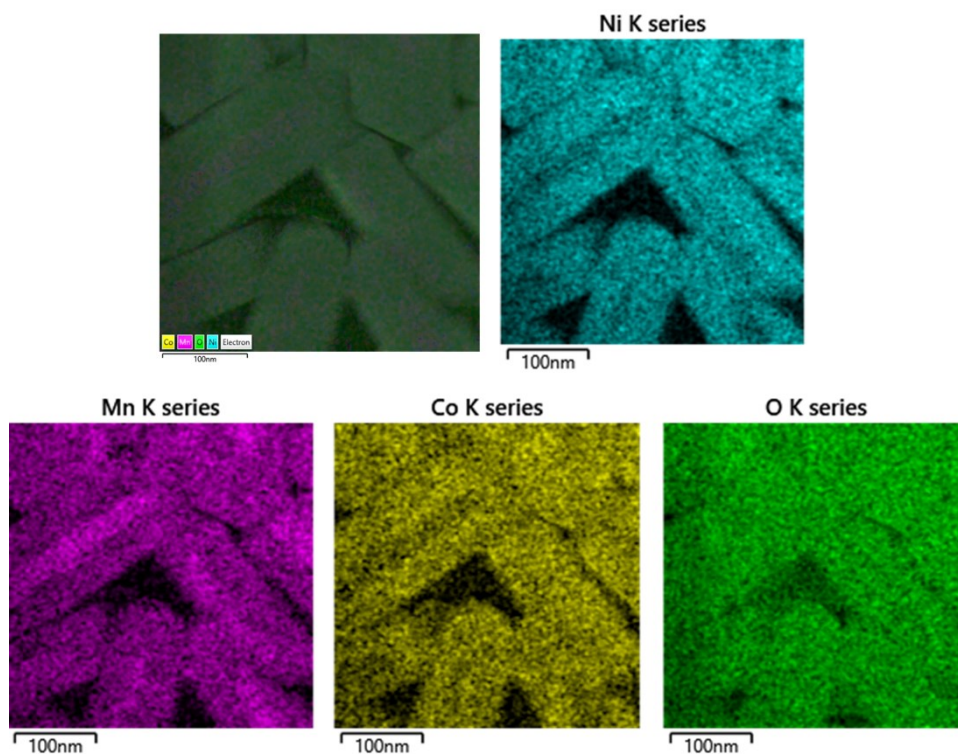
Supplementary Fig. 19 The initial charge-discharge profiles of NMC composite cathodes sintered with different B₂O₃ contents: 2 wt.%, and 5 wt.%.



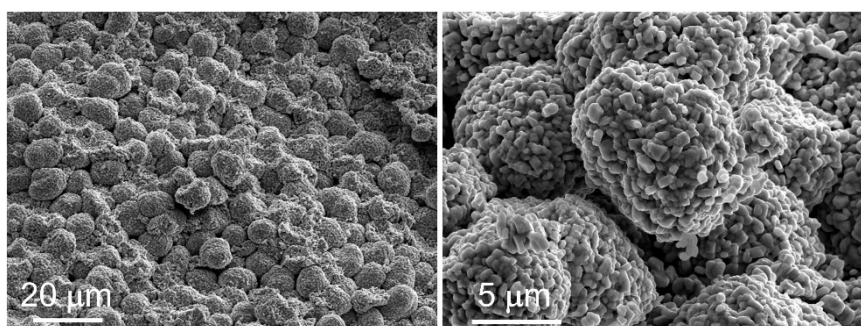
Supplementary Fig. 20 Cross sectional SEM image of the sputtering LATP on NMC622/B₂O₃ (2 wt.%) and corresponding EDS data.



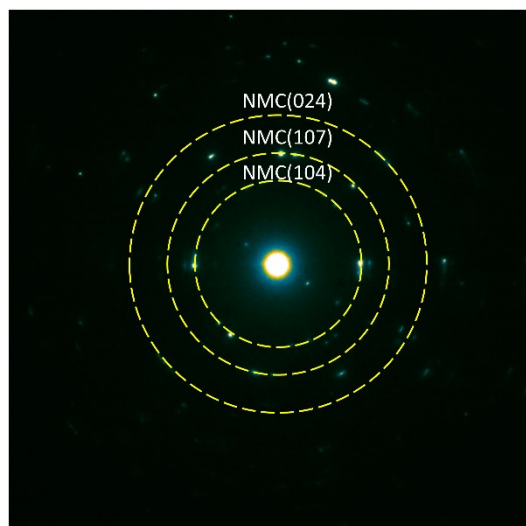
Supplementary Fig. 21 XRD patterns of NMC powders, and sintered NMC cathodes with different contents of B₂O₃ additives.



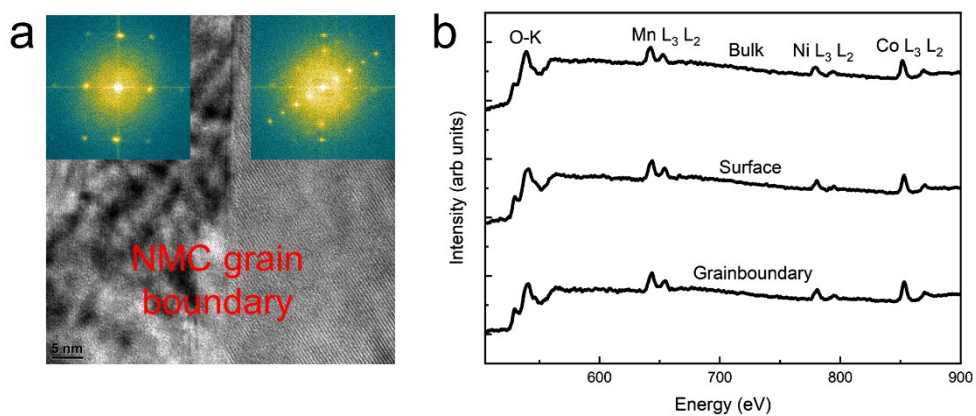
Supplementary Fig. 22 A TEM image of the fractured surfaces of the sintered NMC62/B₂O₃(2 wt.%) cathode and corresponding EDS elemental mappings.



Supplementary Fig. 23 SEM images of the fractured surfaces of the sintered NMC622 cathodes.

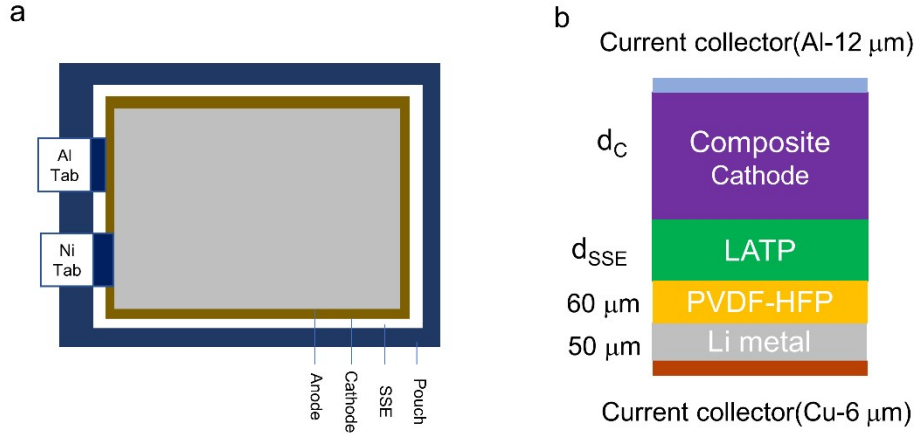


Supplementary Fig. 24 Electron diffraction patterns of the sintered NMC62/ B₂O₃(2 wt.%) cathode.



Supplementary Fig. 25 (a) High resolution TEM image of NMC622 grain boundary in the NMC62/ B₂O₃ (2 wt.%) cathode. (b) EELS at the bulk, surface, and grain boundary of NMC62/ B₂O₃ (2 wt.%) cathode.

Energy density calculations of the LATP-based SSBs.



Supplementary Fig. 26 (a) The configuration of a LAMP-based pouch SSBs. (b) Cross sectional view of all components.

The energy density is calculated based on the above SSB configuration, which contains the pouch (included tabs), the Al foil (12 μm), the composite cathodes (LABTP/LCO or NMC622/B₂O₃), the LATP SSE, the PVDF-HFP gel electrolyte, and the Li metal (50 μm) on copper foil (6 μm). In general, the energy density of a SSB is the energy density of composite cathode divided by the total mass. The SSB energy density can be described as

$$E_{SSE} = \frac{C_c \times V_c \times \rho_c \times d_c \times R}{m_{pouch} + \rho_{Al} \times d_{Al} + \rho_{Cu} \times d_{Cu} + \rho_c \times d_c + \rho_{SSE} \times d_{SSE} + \rho_{Gel} \times d_{Gel} + \rho_{Li} \times d_{Li} + \rho_{Cu} \times d_{Cu}}$$

in which the pouch size and weight is 4.5×3.6 cm² and 1.24 g, respectively; the total weight of Al and Ni tabs is 0.24 g; C_c is the capacity of the composite cathode (110 mAh g⁻¹ for LABTP/LCO-200 μm , 90 mAh g⁻¹ for LABTP/LCO-300 μm , and 170 mAh g⁻¹ for NMC622/B₂O₃); V_c is the average working voltage of the composite cathodes (3.9 V for LABTP/LCO, and 3.7 V for NMC622/B₂O₃); ρ_c is the density of the composite cathodes (3.4 g cm⁻³ for LABTP/LCO, and 4.3 g cm⁻³ for NMC622/B₂O₃); d_c is the thickness of the composite cathode; R is the ratio of active materials (70 % for LABTP/LCO, and 98% for NMC622/B₂O₃) in the composite cathodes; ρ_{Al} is the density of the Al current collector (2.7 g cm⁻³); d_{Al} is the

thickness of the Al current collector (12 μm); ρ_{SSE} is the density of LATP layer (2.98 g cm^{-3}); d_{SSE} is the thickness of the SSE layer; ρ_{Gel} is the density of the PVDF-HFP gel electrolyte (1.0 g cm^{-3}); d_{Gel} is the thickness of the PVDF-HFP layer (60 μm); ρ_{Li} is the density of the Li metal (0.53 g cm^{-3}); d_{Li} is the thickness of the Li metal (50 μm); ρ_{Cu} is the density of copper current (8.96 g cm^{-3}); and d_{Cu} is the thickness of the Cu current collector (6 μm). Take NMC622/B₂O₃ as an example, the details are shown in Table 2,

		Calculation	Weight	Energy
Cathode	NMC622/B ₂ O ₃ (2wt.%) 120 μm thick	$4.3\text{g/cm}^3 \times 0.012\text{cm} \times 5.4\text{cm} \times 3.6\text{cm} \times 2 \times 10$ layers	20.062 g	
	12 μm Al foil	$2.7\text{g/cm}^3 \times 0.0012\text{cm} \times 5.4\text{cm} \times 3.6\text{cm} \times 11$ layers	0.693 g	
	Capacity	170 mAh/g \times 20.062g		3.41 Ah
LATP SSE	50 μm thick	$2.95\text{g/cm}^3 \times 0.005\text{cm} \times 5.4\text{cm} \times 3.6\text{cm} \times 2 \times 10$ layers	5.74 g	
PVDF-HFP	60 μm thick	$1\text{g/cm}^3 \times 0.0060\text{cm} \times 5.4\text{cm} \times 3.6\text{cm} \times 2 \times 10$ layers	2.33 g	
Anode	50 μm Li	$2.53\text{g/cm}^2 \times 5.55\text{cm} \times 3.75\text{cm} \times 2 \times 10$ layers	1.053 g	
	6 μm Cu foil	$8.9\text{g/cm}^3 \times 0.0006\text{cm} \times 5.55\text{cm} \times 3.75\text{cm} \times 10$ layers	1.111 g	
Package foil	115 μm	1.24 g	1.24 g	
Tab	one pair	Ni tab and Al tab	0.23 g	
Voltage				3.7 V
Energy				12.617 Wh
Total weight			32.459	
Specific Energy		20 layers	388 Wh/Kg	

Supplementary Table 2 The energy density calculations of the NMC622/B₂O₃(2wt.%) cathode sealed in a pouch cell (20 layers).